

# Actin dynamics in lamellipodia of migrating border cells in the *Drosophila* ovary revealed by a GFP-actin fusion protein

Vladislav V. Verkhusha<sup>a,\*</sup>, Shoichiro Tsukita<sup>a,b</sup>, Hiroki Oda<sup>a</sup>

<sup>a</sup>*Tsukita Cell Axis Project, ERATO, JST, Kyoto Research Park, Minami-machi, Chudoji, Shimogyo-ku, Kyoto 600-8813, Japan*

<sup>b</sup>*Department of Cell Biology, Faculty of Medicine, Kyoto University, Yoshidakonoe-cho, Sakyo-ku, Kyoto 606-01, Japan*

Received 15 January 1999

**Abstract** Directional migration of border cells in the *Drosophila* egg chambers is a developmentally regulated event that requires dynamic cellular functions. In this study, the electron microscopic observation of migrating border cells revealed loose actin bundles in forepart lamellipodia and numerous microvilli extending from nurse cells and providing multiple adhesive contacts with border cells. To analyze the dynamics of actin in migrating border cells in vivo, we constructed a green fluorescent protein-actin fusion protein and induced its expression in *Drosophila* using the GAL4/UAS system. The green fluorescent protein-actin was incorporated into the actin bundles and it enabled visualization of the rapid cytoskeletal changes in border cell lamellipodia. During the growth of the lamellipodia, the actin bundles that increased in number and size radiated from the bundle-organizing center. Quantification of the fluorescence intensity showed that an accumulation of bundle-associated and spotted green fluorescent protein-actin signals took place during their centripetal movement. Our results favored a treadmilling model for actin behavior in border cell lamellipodia.

© 1999 Federation of European Biochemical Societies.

**Key words:** Green fluorescent protein-actin fusion; Border cell migration; Actin dynamics; Forepart lamellipodium

## 1. Introduction

Directional migration of cells is observed in developing tissues of multicellular organisms. This migration, which is thought to be coordinated with the dynamics of the actin-based cytoskeleton, is developmentally regulated. Studies on cell migration and actin dynamics have been performed using a variety of cells including cultured fibroblasts and keratocytes of vertebrates [1,2] and neural cells of *Aplysia* [3]. Little, however, is known about the dynamic behavior of actin in living cells that are migrating within developing tissues.

In the egg chamber of the *Drosophila* ovary, a small cluster of 6–10 specialized somatic follicle cells, called border cells (BCs), migrates through nurse cells. At stage 9 of oogenesis, BCs break from the anterior follicle epithelium, acquire a mesenchymal-like morphology and migrate posteriorly more than 100  $\mu\text{m}$  for 5–6 h through the nurse cells (NCs) to the oocyte [4]. This BC migration is developmentally and genetically regulated [5]. Several genes have been analyzed which play roles in the regulation of BC differentiation and migration. These include *slow border cells*, *breathless*, *discs large* and

genes encoding small GTPases of the Rho family [6], protein kinase A [7], Ras aggreon fluorescent protein and Rac [8]. Also, mutations in *shotgun* and *armadillo*, which encode DE-cadherin and the *Drosophila* homologue of  $\beta$ -catenin, respectively, affect cell-cell adhesion and the cytoskeletal organization in egg chambers [9,10], resulting in a defective BC migration.

In recent years, a green fluorescent protein derived from the jellyfish *Aequorea victoria* [11,12] has been utilized to visualize the protein behavior and cytoskeletal dynamics in living cells and tissues [13]. It has been shown that in *Saccharomyces cerevisiae* an actin-green fluorescent protein (GFP) fusion protein integrates into cortical actin patches that move in an energy-dependent manner [14]. In undeveloped single cells of *D. discoideum* [15] and in cultured B16F1 melanoma cells [16], a GFP-actin allowed the visualization of a cytoplasmic network and bundles of filamentous actin. Moreover, the GFP-actin construct was able to copolymerize with endogenous actin in vitro and was capable of generating a continuous force in microfilaments containing up to 20% fusion protein [15].

In this study, we observed the morphology of the actin-based cytoskeleton in lamellipodia of migrating BCs in the *Drosophila* ovary by transmission electron microscopy and examined the dynamic changes in patterns of the actin cytoskeletal network using a GFP-actin fusion protein. Our results revealed the growth process of lamellipodia during migration and allowed us to characterize the behavior of actin in the BC lamellipodia.

## 2. Materials and methods

### 2.1. *Drosophila* stocks

GAL4-c306 was used as a driver specific to BCs [8,17]. *arm-GAL4* (J.P. Vincent, Medical Research Council, UK) was used for the ubiquitous expression in embryos. Oregon R was used as a wild-type control.

### 2.2. Genetic technique

For the preparation of the GFP-actin fusion construct, the pRmHa-3 plasmid [18] was digested with *EcoRI* and *KpnI*, and PCR-amplified cDNA of GFP (Quantum Biotechnologies) lacking a stop codon was introduced into pRmHa-3 resulting in pRmHa-3-GFP. A 1.2 kb *KpnI*–*BamHI* fragment encoding the *Drosophila* actin 5C cDNA [19] with an additional 15 nucleotides in the upstream region was amplified by PCR from a *Drosophila* 5' stretch larval cDNA library (Clontech) using the forward primer (GGTACCG-CATCAGCAATGTGTGACGAAGAAGTTGCT) and reverse primer (GGATCCTTAGAAGCACTTGCGGTGCAC). The amplified product was cloned downstream of the GFP sequence in pRmHa-3-GFP resulting in cDNA encoding a fusion protein, GFP-Gly-Thr-Ala-Ser-Ala-actin. Then, the 1.9 kb *EcoRI*–*BamHI* fragment of the GFP-actin cDNA was transferred to the pUAST vector [20] to form pUAST-GFP-actin. This plasmid was microinjected into *w<sup>1118</sup>*; *D2-3 TM3 Sb/Dr* [21] to produce transgenic flies. One established line, UAS-GFP-actin #2-2, was used in this study. This line had one

\*Corresponding author. Fax: (81) (75) 315-9044.  
E-mail: vverkhush@cell.tsukita.jst.go.jp

**Abbreviations:** BC, border cell; NC, nurse cell; GFP, green fluorescent protein; BOC, bundle-organizing center; BDM, 2,3-butanedione monoxime

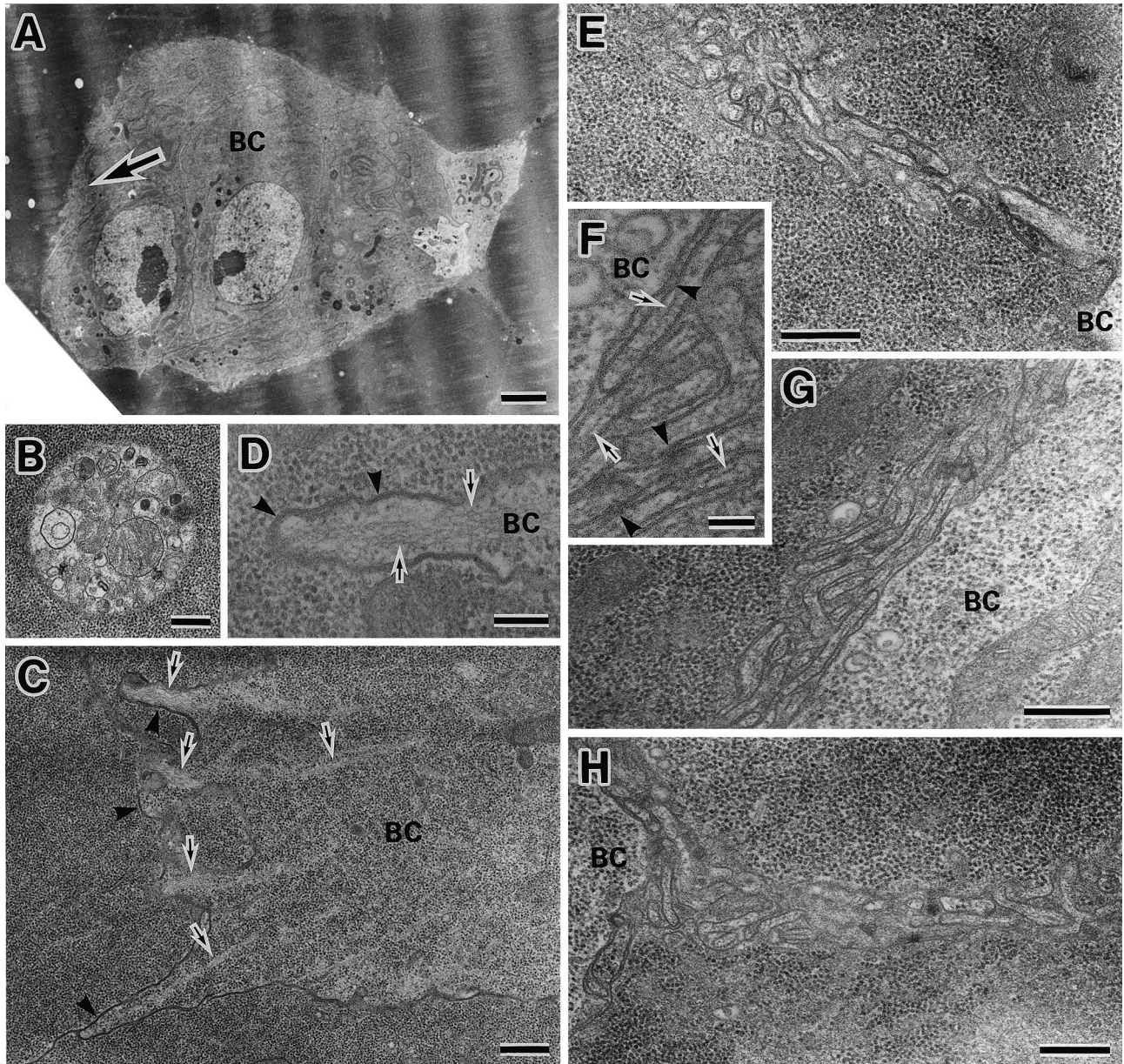


Fig. 1. Transmission electron microscopy of migrating BCs in the *Drosophila* egg chamber. A: The whole cluster of BCs. The thick arrow indicates the direction of BC migration through surrounding NCs. B: One of the multi vesicular bodies which were highly enriched in migrating BCs. C, D: Forepart lamellipodium of migrating BCs extended forward between the NCs. Thin arrows indicate loose actin bundles. Arrowheads indicate tight contacts between forepart BC and the NCs. E–H: Multiple microvilli in the front part (E), at the lateral side (F, G) and behind (H) a migrating BC cluster. Microvilli contained actin filaments (F, arrows) and exhibited spotted contacts with BCs as well as with each other (F, arrowheads). Bars, 2  $\mu\text{m}$  (A), 400 nm (C, E, G, H), 100 nm (B, D, F).

copy of the transgene on the second chromosome. The expression of the GFP-actin targeted to BCs was achieved with the GAL4/UAS gene expression system [20].

### 2.3. Western blotting

Western blotting was performed as previously described [22]. Anti-GFP polyclonal antibodies (Clontech) and anti-actin C11 polyclonal antibodies (Sigma) were used. HRP-conjugated donkey anti-rabbit antibodies (Amersham) were used as secondary antibodies.

### 2.4. Electron microscopy

The fixation and sectioning of egg chambers were performed as previously described [23]. Ultrathin sections were analyzed using a JEM1010 transmission electron microscope.

### 2.5. Fluorescence microscopy and image processing

Actin staining of egg chambers by rhodamine-phalloidin (Molecular Probes) was performed as described [9]. Stained samples were analyzed using a Bio-Rad laser scanning confocal unit (MRC1024) attached to a Zeiss Axiophot microscope. Video images of freshly isolated egg chambers cultured in R-14 medium [24] were acquired by Delta Vision (Applied Precision) using a cooled CCD camera (Photometrics) attached to an inverted fluorescence microscope (Olympus, IX70). All data were collected at  $25 \pm 1^\circ\text{C}$  within 30 min after dissection of flies. Cytochalasin D and 2,3-butanedione monoxime (BDM) were purchased from Sigma. Digitized images of optical sections were applied to deconvolution processing [25] using DeltaVision API software. Further, images were quantitatively analyzed using Quantum Image and assembled in Adobe Photoshop.

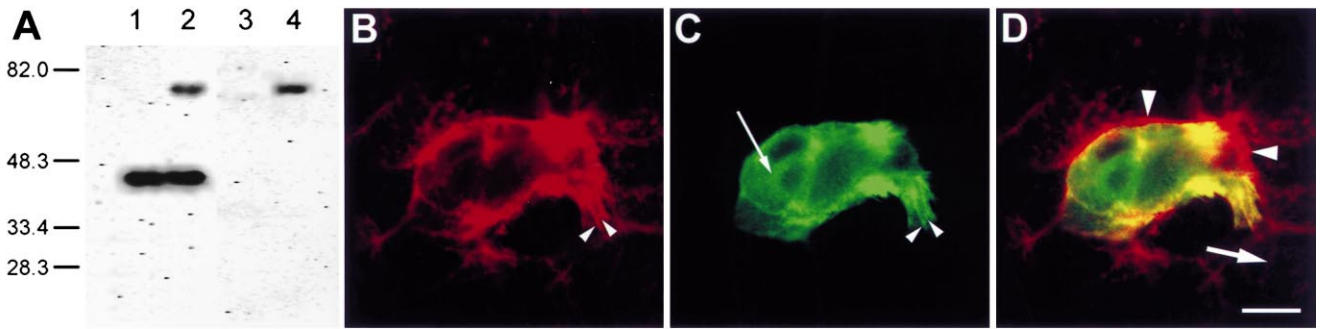


Fig. 2. Expression of the GFP-actin fusion protein in *Drosophila*. A: Western blot of GFP-actin in wild-type embryos (lanes 1, 3) and transgenic embryos expressing GFP-actin (lanes 2, 4) detected by anti-actin (lanes 1, 2) and anti-GFP (lanes 3, 4) Abs, respectively. B–D: Confocal images of BCs expressing the GFP-actin fusion protein. Staining with rhodamine-phalloidin (B), GFP-actin signal (C) and both images superimposed (D) are shown. Cytoplasmic GFP-actin signal is indicated by a thin arrow (C). Small arrowheads indicate spots of filamentous actin on and outside of actin bundles in BC lamellipodium (B, C). NC cortexes exhibited high levels of rhodamine-phalloidin staining at the contacts between NCs and BCs (large arrowheads, D). The direction of BC migration is indicated by a short thick arrow (D). Bar, 10  $\mu$ m.

3. Results and discussion

We examined the morphology of BCs migrating through NCs by transmission electron microscopy. BCs were less electron dense than surrounding NCs and represented a tightly packed cell cluster (Fig. 1A). Multi vesicular bodies, observed previously [10], were markedly enriched in migrating BCs as compared to other follicular cells in the egg chamber (Fig. 1B). Some BCs located at the forefront of the cluster, extended lamellipodia. In the lamellipodia, bundles consisting of loosely associated fine actin filaments were observed (Fig. 1C,D). Most actin bundles were 70–90 nm in diameter and ran straight in centripetal directions in lamellipodia. In some BCs, mats consisting of actin filaments were found and these ranged up to 200 nm in size (data not shown). Lamellipodia, which seemed to be extending forward between NCs, exhibited continuous tight adhesive contacts with the NCs (Fig.

1C,D). Electron microscopy also revealed numerous microvilli extending from NCs (Fig. 1E–H). These microvilli were 60–90 nm in width and 400–800 nm in length. Up to five layers of microvilli were observed between cell bodies of BCs and NCs. On lateral parts of the BC cluster, microvilli of NCs were preferentially oriented parallel to the direction of migration although both microvilli in forward and in backward directions were found (Fig. 1G). Microvilli contained one or a few fine filaments, presumably consisting of polymerized actin, and exhibited multiple spotted contacts with BCs as well as with each other (Fig. 1F). Microvilli found just in front of the forefront lamellipodia of the BC cluster were oriented in various directions (Fig. 1E). Microvilli were also distributed in patchwork patterns along the future route of BCs toward the oocyte (data not shown).

To examine the dynamic aspects of the lamellipodia of migrating BCs, we constructed a GFP-actin fusion protein.

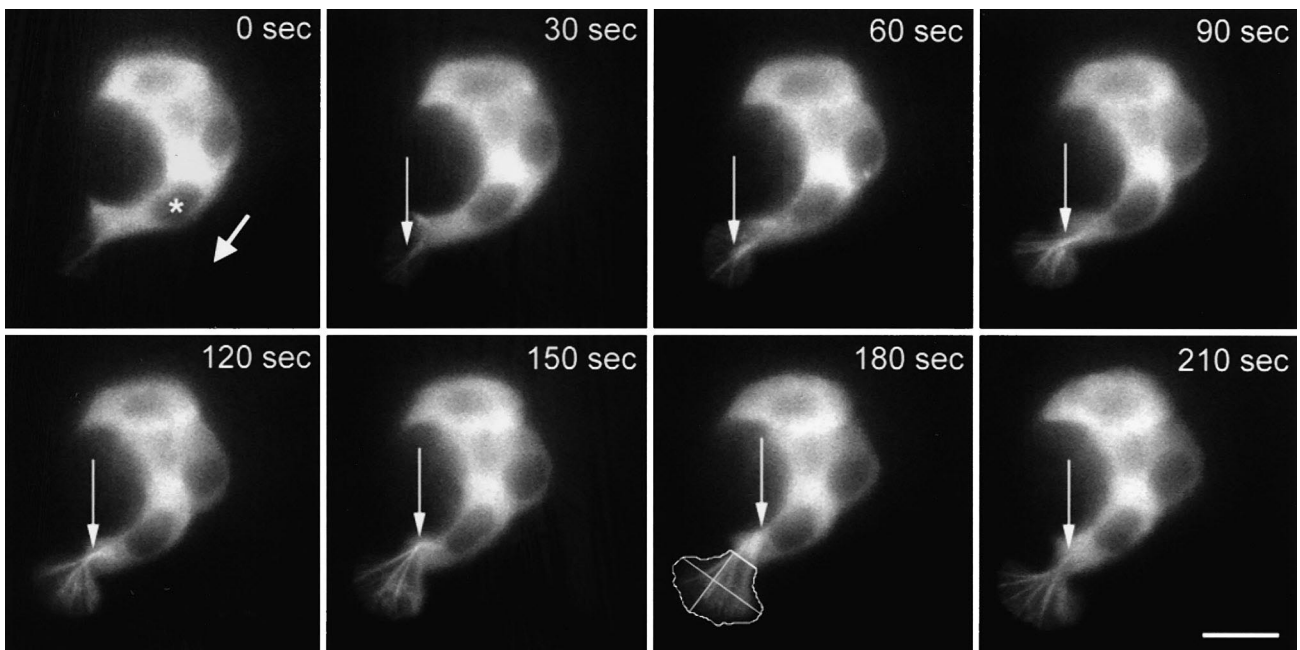


Fig. 3. Lamellipodium growth visualized by the GFP-actin fusion protein. Successive images were taken at the indicated times. The short thick arrow in the first image indicates the direction of migration. Thin arrows indicate the BOC. Nucleus of the forefront BC indicated by a star in the first image. The length and width of BC lamellipodium were measured as indicated at 180 s (see legend for Fig. 4A). Bar, 10  $\mu$ m.

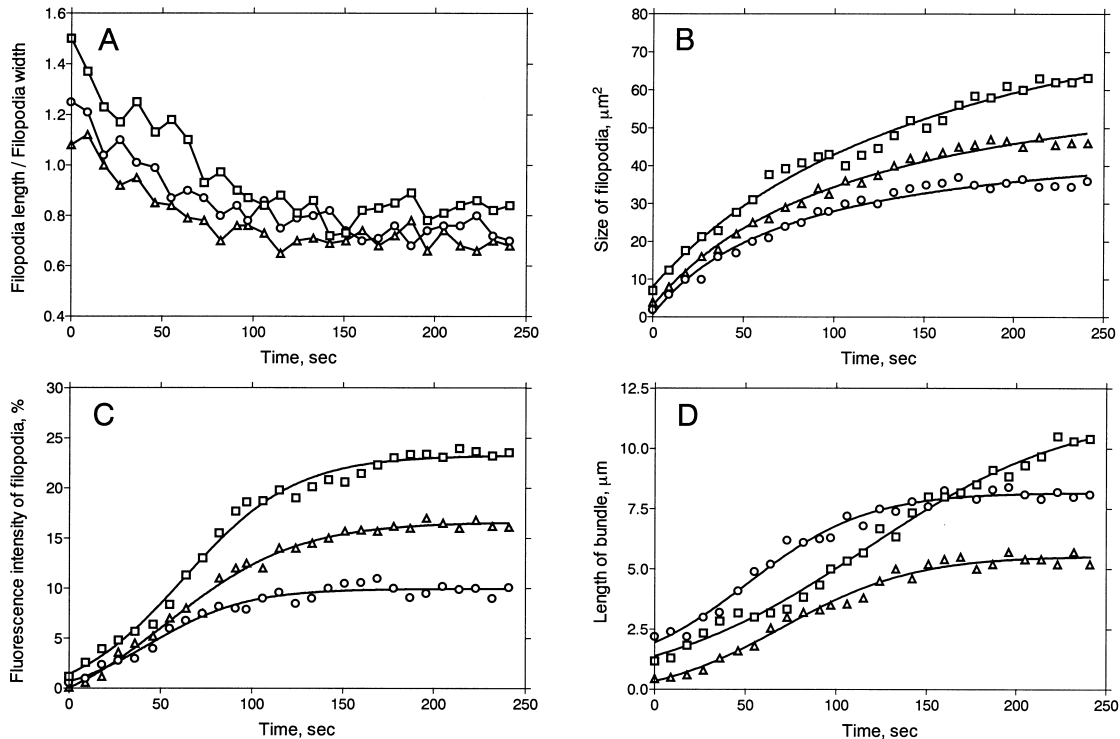


Fig. 4. Spatial and temporal behavior of the GFP-actin in growing lamellipodia of BCs. Squares, circles and triangles represent characteristics measured on optical sections of the forepart lamellipodia in three different BCs. The same symbol represents the same lamellipodium in all panels. A: The extent of temporal changes in profile of lamellipodia is presented as the time course for the ratio between lamellipodia length and width. The length was taken perpendicular to the direction of the lamellipodium neck, extended from the point where the lamellipodium joins the cell body to the edge of the lamellipodium undergoing the largest excursion (as shown in Fig. 3 at 180 s). The width of the lamellipodium was measured perpendicular to the length in the widest part of the lamellipodium. B: Spatial changes in lamellipodia during their growth are displayed as the time course of changes in the size of the same optical section for each lamellipodium. C: Increase of the GFP-actin fluorescent intensity of lamellipodia normalized per total intensity of the respective cell. D: Elongation of actin bundles is presented as the time course of changes in the length of a particular bundle in three different lamellipodia. The length was measured as the distance between the distal and proximal ends of a bundle.

Western blotting analysis of the lysate from embryos expressing GFP-actin revealed the expression of a 70 kDa protein detected both with anti-actin and with anti-GFP antibodies as well as endogenous 42 kDa actin molecules detected only with anti-actin antibodies (Fig. 2A). The size of the GFP-actin was consistent with the expected molecular mass (69.5 kDa). The amount of GFP-actin fusion protein expressed in the embryos was about 15–20% of that of the total endogenous actin. Embryos expressing GFP-actin as well as wild-type embryos showed the 42 kDa endogenous actin band at the same level of expression, indicating that expression of the fusion protein did not influence the expression of endogenous actin.

We induced the expression of GFP-actin using the GAL4-c306 strain and detected fluorescence of GFP-actin in BCs and anterior polar follicle cells but not in most other follicle cells and NCs. In the BCs, GFP-actin was seen in cortical and cytoplasmic regions (Fig. 2B–D). The population of GFP-actin, which was rather uniformly distributed in the cytoplasm, was likely to be monomeric (Fig. 2C). In addition to the cytoplasmic signals, bright GFP-actin fluorescence was observed at the cellular cortex and in lamellipodia. In superimposed images, areas of high GFP-actin accumulation were coincident with intense phalloidin labelling (Fig. 2D). In lamellipodia at the forepart of the BC cluster, some signals for GFP-actin, which were coincident with phalloidin staining, were seen as lines presumably corresponding to actin bundles

observed by electron microscopy. These results suggested that GFP-actin was polymerized into filaments and incorporated into actin bundles in BC forepart lamellipodia.

Furthermore, targeted expression of GFP-actin to BCs allowed us to distinguish the actin distribution in BCs from that in surrounding NCs (Fig. 2D). The edges of NCs contacting BCs exhibited high levels of accumulation of filamentous actin. As in these areas many microvilli were observed by electron microscopy as shown above (Fig. 1G), the microvilli seemed to contain large amounts of filamentous actin consistent with the electron microscopic observation of fine filamentous structures (Fig. 1F).

Next, we performed time lapse recording of GFP-actin fluorescence in BCs in living isolated egg chambers that were cultured for short time periods. The patterns of GFP-actin fluorescence changed dynamically in forepart lamellipodia of BCs during migration. Forepart lamellipodia exhibited various kinds of behavior including growth, retraction and spatial stationing. We analyzed the growth process of forepart lamellipodia (Fig. 3).

At the beginning of growth, the lamellipodium contained a single relatively thick actin bundle (0 s). This bundle started transverse splitting from the periphery of the lamellipodium, giving rise to multiple side bundles (30–60 s). These bundles converged on a point that we termed the bundle-organizing center (BOC). The BOC was displaced from the distal part of

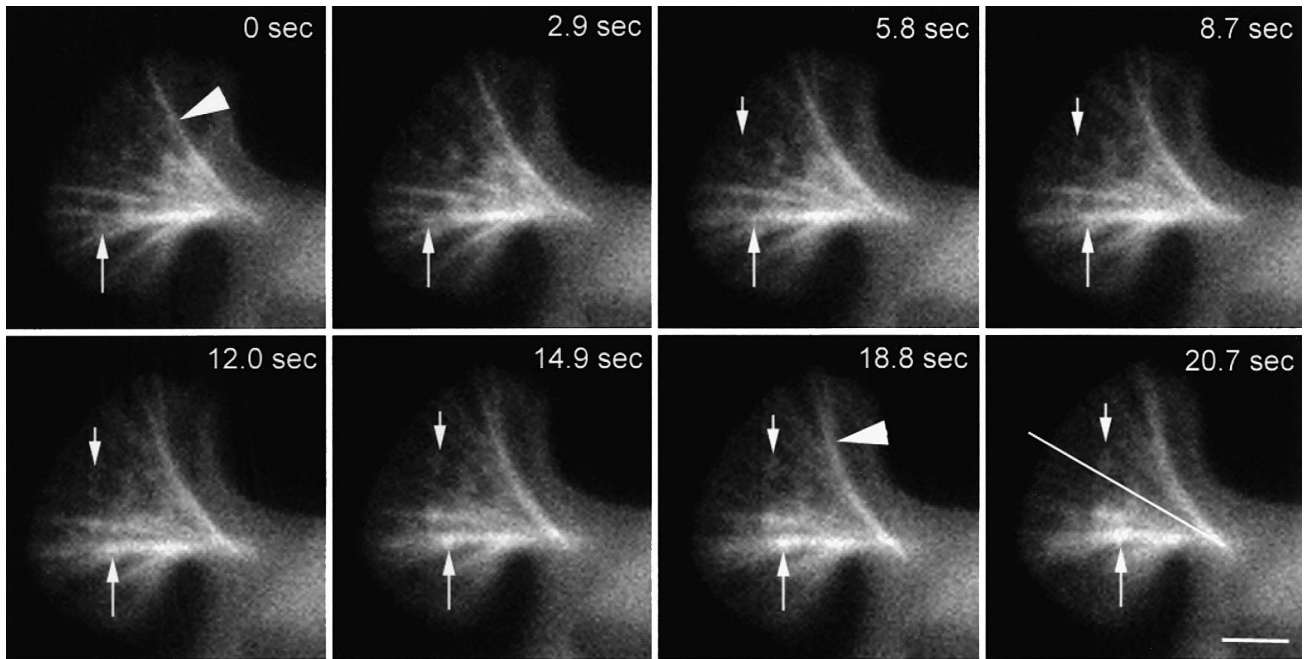


Fig. 5. Fast dynamics of GFP-actin in stationary lamellipodium of BCs. The sequence of still images was taken at the indicated times. Long and short thin arrows indicate the spots of filamentous actin on and outside of the bundle, respectively. Note the side ways displacement of the upper actin bundle (thick arrowheads at 0 and 18.8 s). The thin line in the last image indicates the direction for the measurement of intensity profiles (see Fig. 6A). Bar, 5  $\mu\text{m}$ .

the lamellipodium toward the nucleus coinciding with development of actin bundles. As the BOC moved centerpetally, actin bundles increased in number and size and the lamellipodium widened its peripheral area (60–120 s). Concomitantly, the lamellipodium and cell body became spatially separated by a neck part, giving rise to a hand-like pattern of the actin bundle network. Passing through the neck, the BOC reached the proximal vicinity of the nucleus (150–180 s). Eventually, the BC lamellipodium entered a stationary state (210 s). Although the BOC became separated from the nucleus, it still remained in the cell body.

In the growth phase, the size of lamellipodia increased with repetitive fluctuations and finally reached a stationary plateau (Fig. 4B). The time course of the ratio between lamellipodium length and width indicated that changes of lamellipodia in shape during the growth phase were remarkably large (Fig. 4A). The length/width ratio decreased in parallel with enlarge-

ment of peripheral areas of lamellipodia. Its values changed from 1.0–1.5 to 0.65–0.85. Changes in the total fluorescent intensity of GFP-actin in lamellipodia paralleled changes in the lamellipodium size (Fig. 4C). Actin bundles exhibited a gradual growth up to 5–12  $\mu\text{m}$  (Fig. 4D) resulting in an increase in the distance between the lamellipodium distal edge and the BOC.

To determine the origin of the lamellipodium dynamics, the actin polymerization-blocking drug cytochalasin D (40 ng/ml) or low affinity myosin agonist BDM (200 ng/ml) was added to the culture medium during video recording. Shape changes and growth of lamellipodia were inhibited within 20–30 s by cytochalasin D but not by BDM (data not shown) indicating that the lamellipodium motility was mainly due to actin polymerization.

In the stationary phase of lamellipodium behavior, actin was organized in bundles and in spot-like particles as visual-

Table 1  
Quantitative parameters of GFP-actin dynamics and the lamellipodia motility in BCs<sup>a</sup>

Measured Parameter	Value (SD; <i>n</i> ) <sup>b</sup>
Average values for stationary lamellipodia	
Rate of increase of fluorescence intensity along bundles	0.041%/sec (0.022; 6) <sup>c</sup>
Rate of increase of fluorescence intensity outside bundles	0.019%/sec (0.010; 6) <sup>c</sup>
Rate of GFP-actin transfer throughout whole lamellipodium	0.64%/sec (0.19; 6) <sup>c</sup>
Velocity of centripetal movement of GFP-actin	0.24 $\mu\text{m}/\text{sec}$ (0.072; 12)
Maximal values for growing lamellipodia	
Rate of increase of lamellipodia size	3.9 $\mu\text{m}^2/\text{sec}$ (1.2; 6)
Rate of increase of total fluorescence intensity in lamellipodia	0.26%/sec (0.069; 6) <sup>d</sup>
Rate of lamellipodia lengthening	0.048 $\mu\text{m}/\text{sec}$ (0.021; 6)
Rate of lamellipodia widening	0.077 $\mu\text{m}/\text{sec}$ (0.029; 6)
Elongation rate of actin bundles	0.046 $\mu\text{m}/\text{sec}$ (0.021; 12)
Velocity of side ways displacement of actin bundles	0.091 $\mu\text{m}/\text{sec}$ (0.043; 6)

<sup>a</sup>All calculations were performed for two dimensional projections of lamellipodia on optical sections.

<sup>b</sup>SD, standard deviation of value; *n*, number of objects analyzed.

The values were normalized per fluorescence intensity of respective whole lamellipodium<sup>(c)</sup> or forepart BC<sup>(d)</sup>.

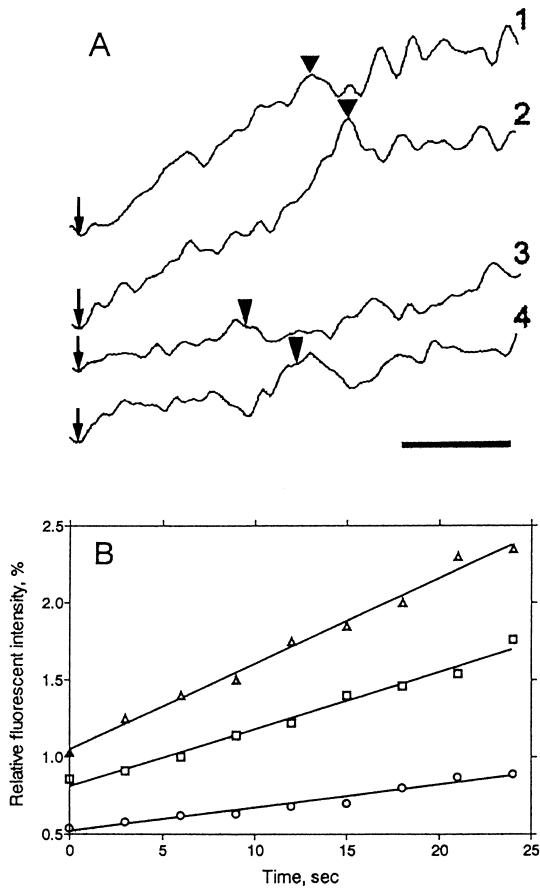


Fig. 6. The spatial and temporal behavior of GFP-actin in a stationary lamellipodium of BCs. A: Typical centripetal profiles of GFP-actin fluorescence taken from the periphery of the same lamellipodium (indicated by arrows at the left side) in the direction to BOC (as indicated on Fig. 5 at 20.7 s). The profiles were measured along (1, 2) and outside (3, 4) of visible bundles at times 0 (1, 3) and 10 s (2, 4), respectively. Short and long arrowheads indicate the positions of two visible GFP-actin spots at times 0 and 10 s, respectively. Bar, 5  $\mu\text{m}$ . B: The increase of fluorescent intensity in three different areas of the same size in a typical lamellipodium during centripetal displacement of GFP-actin. The areas containing a visible GFP-actin spot on bundle (triangles), visible spot outside of bundle (squares) or without any visible particles (i.e. background areas, circles) were selected. The average fluorescent intensity within each area was normalized per current intensity of the whole lamellipodium.

ized by GFP-actin (Fig. 5). Spotted patterns of GFP-actin signals, regardless of whether they were or were not associated with bundles, moved toward the BOC. These spots may correspond to local clusters of filamentous actin as revealed by rhodamine-phalloidin staining (Fig. 2A). The average velocity of centripetal movement of GFP-actin signals in BC lamellipodia was 0.24  $\mu\text{m/s}$  (Table 1). This value was much higher than the velocity of BC migration (approximately 0.01  $\mu\text{m/s}$ ). This was analogous to the cell motility and actin dynamics in filopodia of cultured fibroblasts [1] and in growth cones of *Aplysia* [2] after microinjection of fluorochrome caged actin. In contrast, cultured keratocytes exhibited high migration velocities, which were comparable to the velocity of filament movement relative to the cell edge [3].

To further understand the mechanism controlling actin behavior in stationary lamellipodia, we measured the spatial and temporal gradients of GFP-actin fluorescence intensity. The

intensity in centripetal profiles (Fig. 6A), on average, increased linearly with approach to the BOC. This indicated that depolymerization of filamentous actin did not occur at considerable levels in lamellipodia. Moreover, these spatial gradients were much higher along than outside bundles. The visible GFP-actin spots on or outside bundles were followed, and growth rates were measured and compared with that of areas of the same size without visible GFP-actin particles (Fig. 6B). At the same lamellipodium, the highest rate was detected for spots along bundles, a medium rate for spots outside bundles, and the lowest rate for background areas. Considering that the last case represented spatial distribution of monomeric GFP-actin, we suggested that polymerization was occurring throughout the entire area of the lamellipodium as well as at the distal ends of bundles. These findings together with the microscopic observations favor a treadmilling model rather than a nucleation model for the actin turnover [26]. In accordance with this, it seems that actin depolymerization was driven in BOC in the stationary lamellipodium (Fig. 3, 210 s). In the growing lamellipodium, actin depolymerization probably first occurred at the proximal end of the main bundle (Fig. 3, 30–60 s) and later along split proximal bundles (Fig. 3, 90–120 s) where GFP-actin fluorescence was gradually decreasing toward the nucleus. Such a type of dynamic organization for actin filaments has not been reported previously, although resembling cases were observed in fibroblasts [27] and growth cones [28] where treadmilling polymerization occurred at leading edges and depolymerization was distributed over the entire filopodium.

The treadmilling versus nucleation model for actin dynamics in the lamellipodium of BCs is also supported by kinetic arguments. The time necessary for actin turnover in lamellipodium that predicted by the nucleation model is considerably shorter than that predicted by the treadmilling model as a consequence of the polymerization and depolymerization of short filaments rather than single actin molecules [26]. This time has been estimated for lamellipodium of cells typically exhibiting nucleation of filaments, macrophages [29] and keratocytes [3], as 30 s and 23 s, respectively. However, the turnover time for actin in the lamellipodium of BCs, calculated from the average rate of GFP-actin transfer through the whole lamellipodium (Table 1), was 156 s, which is significantly larger than that in the examples of the nucleation model.

**Acknowledgements:** We thank Dr. L. Manseau and Bloomington Stock Center for the *Drosophila* strains, Dr. A. Asano for the critical reading of the manuscript and suggestions, Ms. S. Okajima and Ms. M. Okubo for the technical assistance. We are also grateful to all members of ERATO Tsukita Cell Axis Project for helpful discussions.

## References

- [1] Wang, Y.-L. (1985) *J. Cell Biol.* 101, 597–602.
- [2] Forscher, P. and Smith, S.J. (1988) *J. Cell Biol.* 107, 1505–1516.
- [3] Theriot, J.A. and Mitchison, T.J. (1991) *Nature* 352, 126–131.
- [4] Spradling, A.C. (1993) in: *The Development of Drosophila melanogaster* (Bate, C. and Arias, A.M., Eds.), Vol. 1, pp. 1–70, CSHL Press, New York.
- [5] Montell, D.J. (1994) *Trends Genet.* 10, 59–62.
- [6] Murphy, A.M. and Montell, D.J. (1996) *J. Cell Biol.* 133, 617–630.
- [7] Lane, M.E. and Kalderon, D. (1995) *Mech. Dev.* 49, 191–200.
- [8] Lee, T., Feig, L. and Montell, D.J. (1996) *Development* 122, 409–418.

- [9] Oda, H., Uemura, T. and Takeichi, M. (1997) *Genes Cells* 2, 29–40.
- [10] Peifer, M., Orsulic, S., Sweeton, D. and Wieschaus, E. (1993) *Development* 118, 1191–1207.
- [11] Prasher, D.C., Eckenrode, V.K., Ward, W.W., Prendergast, F.G. and Cormier, M.J. (1992) *Gene* 111, 229–233.
- [12] Chalfie, M., Tu, Y., Euskirchen, G., Ward, W.W. and Prasher, D.C. (1994) *Science* 263, 802–805.
- [13] Ludin, B. and Matus, A. (1998) *Trends Cell Biol.* 8, 72–77.
- [14] Doyle, T. and Bolstein, D. (1996) *Proc. Natl. Acad. Sci. USA* 93, 3886–3891.
- [15] Westphal, M., Jungbluth, A., Heidecker, M., Muhlbauer, B., Heizer, C., Schwartz, J.M., Marriott, G. and Gerisch, G. (1997) *Curr. Biol.* 7, 176–183.
- [16] Ballestream, C., Wehrle-Haller, B. and Imhof, B.A. (1998) *J. Cell Sci.* 111, 1649–1658.
- [17] Manseau, L., Baradaran, A., Brower, D., Budhu, A., Elefant, F., Phan, H., Philp, A.V., Yang, M., Glover, D., Kaiser, K., Palter, K. and Selleck, S. (1997) *Dev. Dyn.* 209, 310–322.
- [18] Bunch, T.A., Grinblat, Y. and Goldstein, L.S. (1988) *Nucleic Acids Res.* 16, 1043–1061.
- [19] Fyrberg, E.A., Bond, B.J., Hershey, N.D., Mixer, K.S. and Davidson, N. (1981) *Cell* 24, 107–116.
- [20] Brand, A.H. and Perrimon, N. (1993) *Development* 118, 401–415.
- [21] Robertson, H.M., Preston, C.R., Phillis, R.W., Johnson-Schlitz, D., Benz, W.K. and Engels, W.R. (1988) *Genetics* 118, 461–470.
- [22] Oda, H., Uemura, T., Shiomi, K., Nagafuchi, A., Tsukita, S. and Takeichi, M. (1993) *J. Cell Biol.* 121, 1133–1140.
- [23] Oda, H., Tsukita, S. and Takeichi, M. (1998) *Dev. Biol.* 203, 435–450.
- [24] Robb, J.A. (1969) *J. Cell Biol.* 41, 876–885.
- [25] Shaw, P. (1994) *Histochem. J.* 26, 687–694.
- [26] Mitchison, T.J. and Cramer, L.P. (1996) *Cell* 84, 371–379.
- [27] Symons, M.H. and Mitchison, T.J. (1991) *J. Cell Biol.* 114, 503–513.
- [28] Lin, C.-H. and Forscher, P. (1993) *J. Cell Biol.* 121, 1369–1383.
- [29] Rinnerthaler, G., Herzog, M., Klappacher, M., Kunka, H. and Small, J.V. (1991) *J. Struct. Biol.* 106, 1–16.